

Potential energy surface discontinuities in local correlation methods

Cite as: J. Chem. Phys. **121**, 691 (2004); <https://doi.org/10.1063/1.1759322>

Submitted: 24 February 2004 . Accepted: 15 April 2004 . Published Online: 24 June 2004

Nicholas J. Russ, and T. Daniel Crawford



View Online



Export Citation

ARTICLES YOU MAY BE INTERESTED IN

[An efficient and near linear scaling pair natural orbital based local coupled cluster method](#)
The Journal of Chemical Physics **138**, 034106 (2013); <https://doi.org/10.1063/1.4773581>

[Fast linear scaling second-order Møller-Plesset perturbation theory \(MP2\) using local and density fitting approximations](#)
The Journal of Chemical Physics **118**, 8149 (2003); <https://doi.org/10.1063/1.1564816>

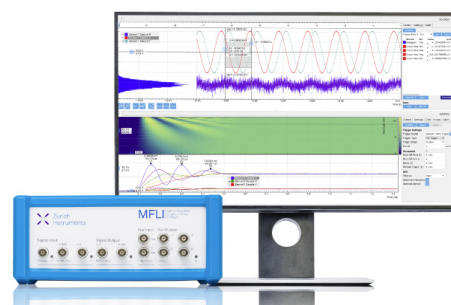
[Gaussian basis sets for use in correlated molecular calculations. I. The atoms boron through neon and hydrogen](#)
The Journal of Chemical Physics **90**, 1007 (1989); <https://doi.org/10.1063/1.456153>

Challenge us.

What are your needs for periodic signal detection?



Zurich
Instruments



Potential energy surface discontinuities in local correlation methods

Nicholas J. Russ and T. Daniel Crawford^{a)}

Department of Chemistry, Virginia Tech, Blacksburg, Virginia 24061

(Received 24 February 2004; accepted 15 April 2004)

We have examined the occurrence of discontinuities in bond-breaking potential energy surfaces given by local correlation methods based on the Pulay–Saebø orbital domain approach. Our analysis focuses on three prototypical dissociating systems: the C-F bond in fluoromethane, the C-C bond in singlet, ketene, and the central C-C bond in propadienone. We find that such discontinuities do not occur in cases of homolytic bond cleavage due to the inability of the Pipek–Mezey orbital localization method to separate singlet-coupled charges on distant fragments. However, for heterolytic bond cleavage, such as that observed in singlet ketene and propadienone, discontinuities occur both at stretched geometries and near equilibrium. These discontinuities are usually small, but may be of the same order of magnitude as the localization error in some cases. © 2004 American Institute of Physics. [DOI: 10.1063/1.1759322]

I. INTRODUCTION

The rigorous computation of the properties of large molecules is one of the great challenges to *ab initio* quantum chemistry. Although hyperaccurate theoretical predictions of various properties of small molecules are now commonplace, the polynomial scaling wall of the most reliable methods such as coupled cluster theory {e.g., the $\mathcal{O}(N^7)$ scaling of the popular coupled cluster singles and doubles plus perturbative triples [CCSD(T)] method} has prevented their routine application to molecules containing more than around ten nonhydrogen atoms. One of the most promising approaches to overcoming the scaling problem is through “local correlation,” which was pioneered by Pulay and Saebø.^{1,2} This idea relies on the fact that electron correlation effects in molecular systems with large band-gaps (insulators) should decrease asymptotically with the interorbital distance as $1/r^6$. By choosing a well-localized form for the molecular orbitals that parametrize the determinantal wave function expansion, one may limit orbital excitations/substitutions to occupied-virtual pairs that are in close proximity. This approach thus reduces the number of independent wave function coefficients one must compute and store, and thus reduces the computational order of the method, perhaps even to linear scaling. The local correlation concept has been applied successfully to many-body perturbation theory^{2–8} and coupled cluster theory.^{9–24} We note, in particular, the recent, impressive developments by Saebø and Pulay on linear-scaling (MP2) calculations with more than 1800 basis functions²⁵ and by Schütz on chains of up to 16 glycine molecules at the local coupled cluster singles and doubles (LCCSD) level of theory.²¹

One of the criticisms leveled at the Pulay–Saebø local correlation concept, however, stems from its dependence upon geometry-specific localization criteria. Specifically, the Pulay–Saebø scheme assigns to each localized occupied molecular orbital (MO) a “domain,” i.e., a group of atoms

whose atomic orbital basis functions (projected onto the unoccupied subspace) serve as that MOs excitation space.² These domains commonly correspond to bonded atoms (e.g., the carbon and oxygen atom participating in a carbonyl π -bond), lone pairs, etc., depending upon the choice of localization criteria for the occupied space. (The Pipek–Mezey charge maximization method is perhaps the most commonly used localization definition.²⁶) Unfortunately, if the molecular structure changes significantly, as in a dissociation or isomerization reaction, for example, the orbital domain structures may change as well, potentially leading to discontinuities in the resulting potential energy surface (PES). The local correlation methods introduced by Scuseria and co-workers,^{7,13} and by Head-Gordon and co-workers,^{6,10–12} have been designed to use atom-based domain structures that are thus geometry-independent. However, the question remains: Do PES discontinuities occur in practical applications of the Pulay–Saebø-based local correlation methods, such as those developed by Werner, Schütz, and co-workers, and, if so, what significance do they have?

The purpose of this work is to investigate these questions using three prototypical systems: the homolytic cleavage of the C-F bond in fluoromethane, CH₃F, and the heterolytic cleavage of the methylene C-C bond in singlet ketene, CH₂CO, and propadienone, CH₂CCO. We have chosen these examples in part because of their small size, but also because the dissociation processes can still be correctly described by single-reference correlation methods such as CCSD and MP2.

II. THEORETICAL BACKGROUND

In the ground-state local correlation approach developed by Pulay and Saebø, the orbital domain structure noted above limits the excitations generated by the cluster/excitation operators in the construction of the determinantal wave function. In the most widely used implementations of the Pulay–Saebø scheme, the occupied orbitals are chosen to

^{a)}Electronic mail: crawdad@vt.edu

be the charge-maximized functions defined by Pipek and Mezey.²⁶ These orbitals are conveniently orthonormal and well-localized in most cases. In the Pulay–Saebø approach, the unoccupied orbitals are defined as the set of nucleus-centered atomic orbitals (AOs), orthogonalized against the occupied space, but nonorthogonal to each other. For a given localized occupied orbital ϕ_i , its virtual domain is chosen as the set of atoms whose associated projected AOs contribute most strongly to the total population of ϕ_i . This choice is implemented in an algorithmic manner using the completeness criterion suggested by Boughton and Pulay²⁷

$$f_i(C') = \min \left\{ \int (\phi_i - \phi')^2 d\tau \right\} \\ = 1 - \sum_{\mu \in [i]} \sum_{\nu} C_{\mu}^{\prime i} S_{\mu\nu} C_{\nu}^i, \quad (1)$$

where ϕ' is the approximation to ϕ_i for the chosen set of AOs ϕ_{μ} , with associated MO coefficients $C_{\mu}^{\prime i}$ and C_{μ}^i , respectively. Thus, the size (i.e., the number of atoms) in the domain of a given occupied orbital is dependent solely on the choice of cutoff of the function $f_i(C')$. A value of 0.02 preserves bonded atoms in well-localized systems and is commonly used for ground-state local-MP2 and local-CCSD calculations.⁹ With the Boughton–Pulay criterion, single excitations out of occupied orbital ϕ_i are allowed only into projected-AO functions associated with those atoms in the orbital's domain. Pairwise excitations from orbitals ϕ_i and ϕ_j are chosen as the union of the orbitals' single-excitation domains, with additional decomposition into “strong” and “weak” pairs to further reduce the scaling of the method.^{2,9}

One drawback to the Pulay–Saebø approach that has been pointed out in the literature^{11,12} is the dependence of the orbital domain structure (and thus the excitation/Fock space on which the wave function is defined) on the molecular structure. If the geometry changes significantly across the PES, e.g., as bonds are broken and formed, the orbital domain structure may change abruptly and a concomitant discontinuity in the PES will appear. Thus, local correlation methods defined in this way cannot adhere to the widely accepted ideal of a “theoretical model chemistry,” defined by Pople.²⁸

On the other hand, Pulay and Saebø have argued convincingly that the changing structure of the correlating space with molecular geometry should be considered a feature of their method. In particular, the local correlation approach may lead to a reduction in intermolecular basis-set superposition error (BSSE),^{29,30} in which the local wave function on one fragment benefits from the presence of AO basis functions on another nearby fragment resulting in overestimation of the computed dimerization energy. BSSE can have a substantial effect on fragmentation energies (approximately 2 kcal/mol or more) and is often reduced using so-called counterpoise corrections.³¹ However, as Pulay and Saebø have discussed, for weakly interacting fragments, their local correlation method limits the intramolecular correlation space of occupied orbitals on a given fragment to (projected) AOs on that same fragment, thus reducing the correlation contribu-

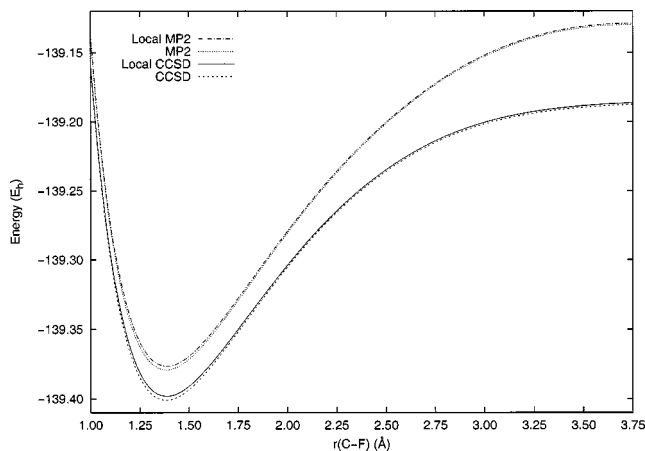


FIG. 1. Canonical- and local-MO MP2 and CCSD potential energy curves (using the cc-pVDZ basis set) for the dissociation of the C-F bond in CH_3F .

tion to the BSSE.³² The same advantage is expected for the Head-Gordon and the Scuseria approaches.

In this work, we seek to answer two important questions: (1) Under what circumstances can PES discontinuities occur in local correlation methods based on the Pulay–Saebø approach? and (2) What are the magnitudes of these discontinuities for typical systems?

III. COMPUTATIONAL DETAILS

Canonical-molecular orbital (MO) and local-MO second-order perturbation theory (MP2)³³ and coupled cluster singles and doubles (CCSD) calculations^{34,35} using spin-restricted orbitals were carried out for fluoromethane CH_3F , singlet ketene CH_2CO , and propdienone CH_2CCO , using the PSI 3 quantum chemical program package.³⁶ The local-CCSD approach we have implemented is a “pilot” program that uses the canonical-MO code to simulate the local correlation treatment. This method was briefly described by Saebø and Pulay in one of their earlier local correlation articles,⁴ and was used by Hampel and Werner in their seminal paper on local-CCSD⁹ and by Crawford and King in a recent extension of these methods to excited states via the local equation-

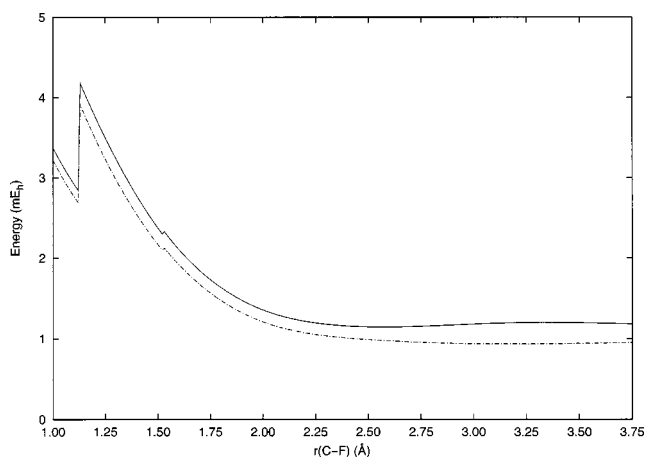


FIG. 2. LMP2 and LCCSD localization errors (in mE_h) for dissociation of the C-F bond in CH_3F . The inner discontinuity corresponds to the expansion of a fluorine lone-pair orbital domain at short bond lengths.

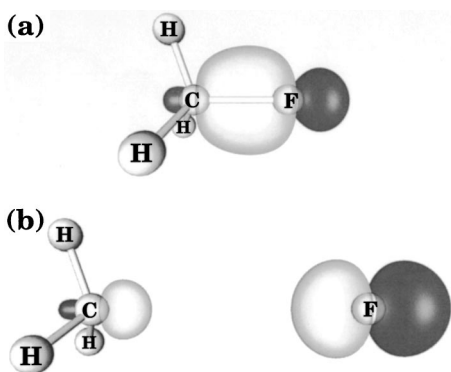


FIG. 3. Contour plots of the Pipek–Mezey localized C-F bonding orbital of CH_3F (a) near the equilibrium geometry and (b) at dissociation.

of-motion (EOM)-CCSD approach.³⁷ No distinction was made between weak and strong pairs in these calculations, i.e., all localized pair domains were treated explicitly in the local-CCSD calculations. Core orbitals were held frozen in all these calculations, and a Boughton–Pulay completeness cutoff of 0.02 was used throughout. The correlation-consistent polarized-valence double-zeta (cc-pVDZ) basis set developed by Dunning was used for all calculations reported here.³⁸

IV. HOMOLYTIC BOND DISSOCIATION: FLUOROMETHANE

Figure 1 plots the conventional and localized MP2 and CCSD potential energy curves for breaking the C-F bond in fluoromethane CH_3F , with all other geometric parameters fixed at their CCSD/cc-pVDZ optimized values. Although this dissociation involves homolytic bond cleavage, the bond in question nominally involves only two electrons. Therefore, the CCSD approach is still capable of providing a qualitatively reasonable potential curve, though CCSD significantly overestimates the well depth.³⁹ On the other hand, the MP2 curve [as well as curves from perturbative methods such as CCSD(T)] will exhibit a characteristic “turnover” at

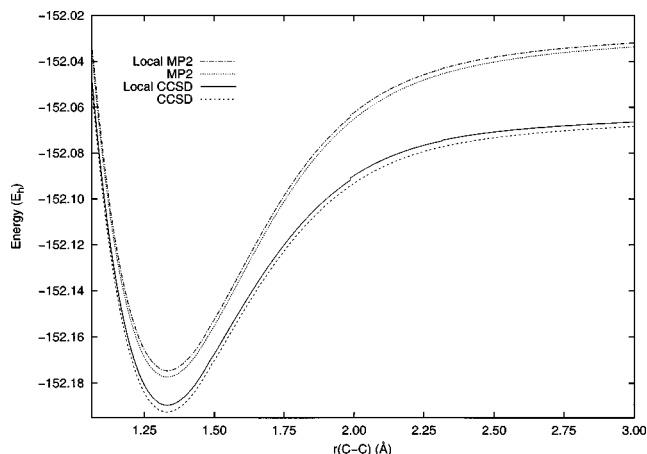


FIG. 4. Canonical- and local-MO MP2 and CCSD potential energy curves (using the cc-pVDZ basis set) for the dissociation of the C-C bond in singlet ketene CH_2CO . The structure was reoptimized at the CCSD/cc-pVDZ level of theory for each value of the C-C bond distance.

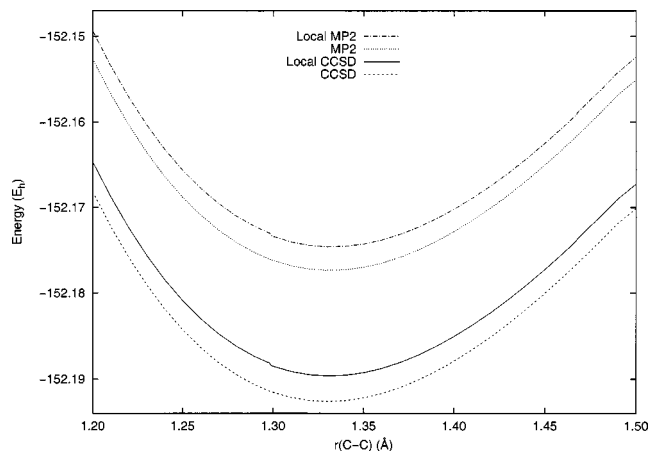


FIG. 5. Closeup of the singlet ketene curves shown in Fig. 4 focused on the near-equilibrium “rearrangement” discontinuities described in the text.

long distances due to the narrowing of the (HOMO-LUMO) gap; the early stages of this phenomenon are already visible in the figure near $r(\text{C-F}) = 3.75 \text{ \AA}$.

The most striking feature of Fig. 1 is that there is clearly *no discontinuity* in either the LMP2 or the LCCSD energy in the bond-breaking region of the potential energy curve, indicating that the orbital domain structure remains constant for long C-F distances. (A discontinuity of about $1.0 mE_h$ occurs at very short C-F distances—less than 1.25 \AA —due to expansion of the domain of a fluorine lone pair to include the carbon atom, as is visible in Fig. 2.) We emphasize that this lack of discontinuity in the dissociation region of the curve is not the result of user-defined constraints on the orbital domains, but instead stems naturally from the inability of the spin-restricted Pipek–Mezey scheme to truly localize the C-F “bonding” MO. Figure 3 illustrates this point: Near equilibrium and at dissociation the Pipek–Mezey localized C-F bonding MO clearly involves AOs on both fragments CH_3 and F. That is, since the electrons in this MO are singlet-coupled and only occupied-orbital mixings are allowed, no charge-localization can occur, and the MO remains delocalized. [We note that, if we had allowed for spin polarization at stretched bond lengths—i.e., if we had followed

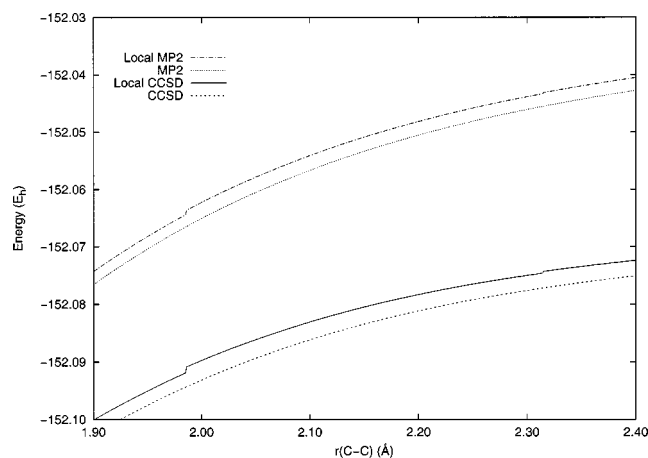


FIG. 6. Closeup view of the singlet ketene curves shown in Fig. 4 focused on the outer π and σ bond-breaking discontinuities described in the text.

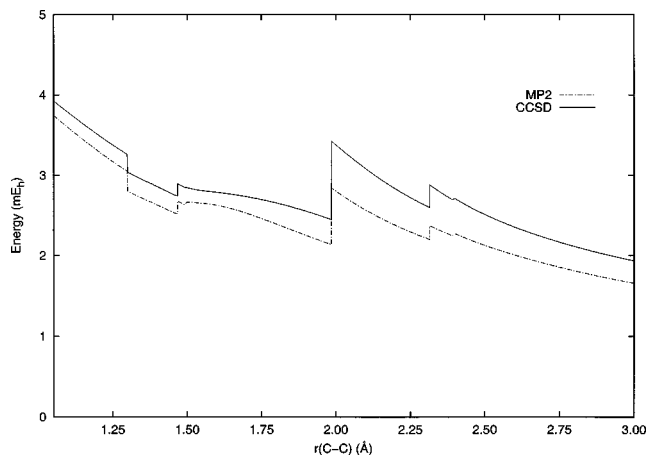


FIG. 7. LMP2 and LCCSD localization errors (in mE_h) for singlet ketene dissociation, where the four discontinuities discussed in the text are clearly visible.

the triplet instability to spin-unrestricted MOs—the Pipek–Mezey procedure would have produced properly localized orbitals, and a discontinuity (*vide infra*) would have appeared.] We may therefore conclude from these results that for *homolytic* bond-breaking, the Pulay–Saebø local-correlation approach will not necessarily lead to discontinuous potential energy surfaces, due to the natural (and appropriate) inability of orbital localization methods such as Pipek–Mezey to separate singlet-coupled charges on distant fragments. We also note that the coupled cluster method (as well as any correlation approach based on a spin-restricted Hartree-Fock wave function) is not size-consistent for this type of bond-breaking process.

V. HETEROLYTIC BOND DISSOCIATION: SINGLET KETENE

Given the above observation of a lack of PES discontinuity for homolytic bond cleavage in the LMP2 and LCCSD methods, we then chose to examine the effect of *heterolytic*

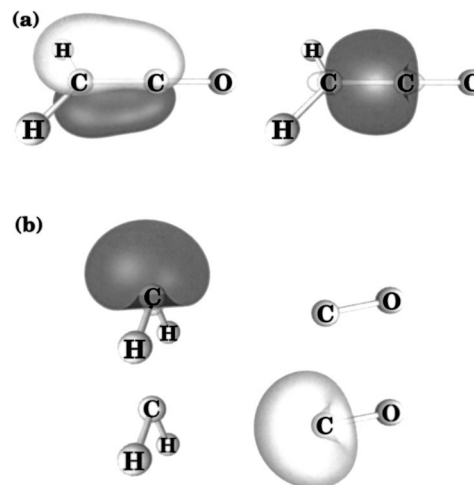


FIG. 8. Contour plots of the relevant Pipek–Mezey localized orbitals for singlet ketene: (a) The π and σ bonding orbitals near the equilibrium geometry and (b) the corresponding lone-pair dissociated MOs of singlet methylene and carbon monoxide.

bond cleavage on the orbital domain structure. The C-C double bond in singlet ketene CH_2CO provides a useful example of this type of dissociation process. This species and its triplet counterpart have been extensively scrutinized both experimentally and theoretically to test the Rice–Ramsperger–Kassel–Marcus (RRKM) behavior of the rate constant for dissociation.^{40–45} It is well known that the lowest singlet surface (i.e., dissociation to singlet methylene and carbon monoxide) proceeds through a C_s -symmetry structure, sometimes referred to in the literature as the C_s^I pathway.^{40,46} We have followed this lowest-energy coordinate to ketene dissociation by computing the optimized CCSD/cc-pVDZ structure for different values of the C-C bond distance. At equilibrium the structure has C_{2v} symmetry, but falls to C_s symmetry as the $\text{C}=\text{C}=\text{O}$ moiety bends up and out of the plane of the molecule near a $r(\text{C}-\text{C})$ bond distance of around 1.49 Å.

TABLE I. Estimates of the sizes of the two LMP2 and LCCSD discontinuities on the dissociation surface of singlet ketene. Localization errors (ΔE) are computed as the difference between the canonical-MO and local-MO methods at the given value of $r(\text{C}-\text{C})$. The discontinuity size is estimated as the difference between the two errors at values of $r(\text{C}=\text{C})$ on either side of the orbital-domain shift. Total energies are given in E_h and energy differences in mE_h .

$r(\text{C}-\text{C})$	MP2			CCSD		
	Canonical	Local	ΔE	Canonical	Local	ΔE
1.298	-0.437156	-0.434105	3.051	-0.452480	-0.449219	3.261
1.299	-0.437208	-0.434404	2.804	-0.452529	-0.449490	3.039
Discontinuity	—	—	-0.247	—	—	-0.222
1.467	-0.445013	-0.442492	2.521	-0.460006	-0.457261	2.745
1.468	-0.445049	-0.442370	2.679	-0.460042	-0.457147	2.895
Discontinuity	—	—	0.158	—	—	0.150
1.985	-0.422345	-0.420210	2.135	-0.450137	-0.447689	2.449
1.986	-0.422290	-0.419450	2.841	-0.450101	-0.446678	3.423
Discontinuity	—	—	0.706	—	—	0.974
2.314	-0.409867	-0.407666	2.201	-0.441556	-0.438958	2.598
2.315	-0.409843	-0.407474	2.369	-0.441540	-0.438662	2.878
Discontinuity	—	—	0.168	—	—	0.280

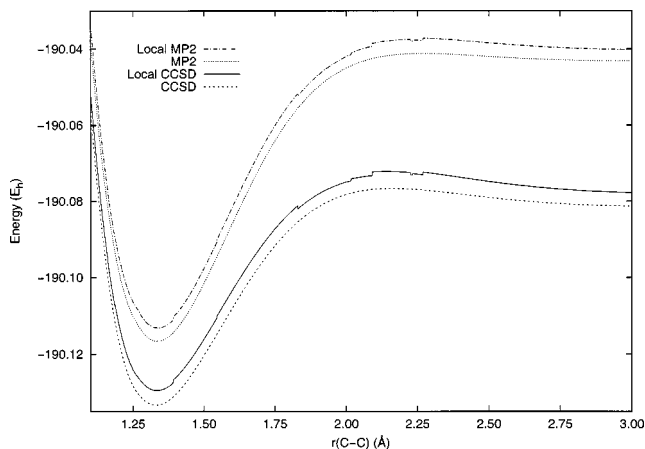


FIG. 9. Canonical- and local-MO MP2 and CCSD potential energy curves (using the cc-pVDZ basis set) for the dissociation of the central C-C bond in singlet propadienone CH_2CCO . The structure was reoptimized at the CCSD/cc-pVDZ level of theory for each value of the C-C bond distance.

Figures 4, 5, and 6 plot the conventional and local MP2 and CCSD potential energy curves for breaking the ketene C-C double bond. Unlike the CH_3F curve, the ketene PES exhibits a total of four discontinuities: two near the equilibrium geometry at approximately 1.298 and 1.467 and two in the dissociation regime at 1.985 and 2.314 Å. These discontinuities are better emphasized by plotting the localization error (i.e., the difference between the canonical and local energies), as shown in Fig. 7. The two inner discontinuities stem from changes in the valence-MO domain structures involving the C=C=O chain, while the two outer discontinuities result from the bond breaking: The cleavage occurs heterolytically, with the part of the $\sigma-\pi$ double bond following the CO fragment and the remaining component following the methylene fragment. The two outer discontinuities appear separately in the curve because the corresponding orbital domain structures change at different points. This process is illustrated in Fig. 8, which plot contour surfaces of the relevant σ and π Pipek–Mezey localized orbitals near equilibrium and at dissociation.

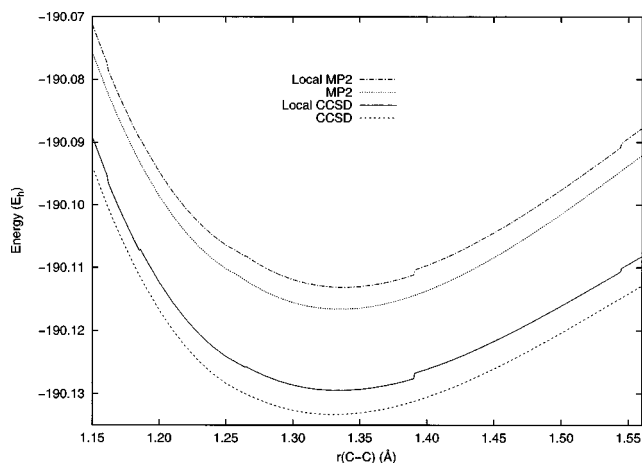


FIG. 10. Closeup of the singlet propadienone curves shown in Fig. 9 focused on the near-equilibrium “rearrangement” discontinuities described in the text.

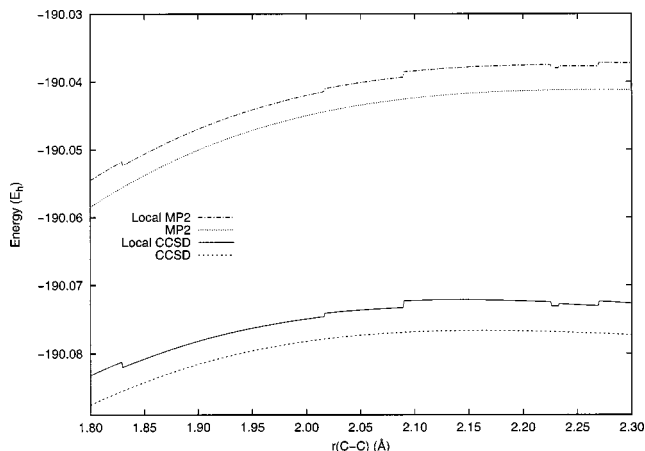


FIG. 11. Closeup of the singlet propadienone curves shown in Fig. 9 focused on the bond-breaking region described in the text.

As shown in Fig. 7 and in Table I, the inner LCCSD discontinuities are small, 0.1–0.2 mE_h , while the outer ones are larger at 0.3–1.0 mE_h , of the same order of magnitude as the localization error (i.e., the difference in the canonical and local CCSD energies). The source of this difference is related to the structure of the orbital domains and the orbital energies. The inner discontinuities stem from rearrangements in the orbital domain structure of the localized HOMO-1, which is a bonding MO on the carbon monoxide; for $r(\text{C}=\text{C})$ value less than 1.298 Å and greater than 1.468 Å, the domain of this MO is limited to projected AOs on the CO moiety, but in between these values the domain includes AOs on the methylene carbon. These changes result naturally from the Boughton–Pulay criterion in Eq. (1). The outer discontinuities, on the other hand, corresponding to actual bond breaking, with the skip at 1.985 Å corresponding essentially to the breaking of the π component of the C-C double bond and the skip at 2.314 Å to the breaking of the σ component. The former discontinuity is larger because it involves the HOMO, while the latter orbital is significantly lower in energy.

VI. HETEROLYTIC BOND DISSOCIATION: PROPADIENONE

As a second test of discontinuities arising in heterolytic bond cleavage, we considered singlet propadienone, CH_2CCO , which is clearly related to ketene, but whose electronic structure is somewhat more complicated by increased conjugation. Unlike ketene, propadienone has C_s symmetry at equilibrium ($r(\text{C}-\text{C}) = 1.34$ Å), with a “kink” in its cumulenyl chain discussed previously by East.⁴⁷ At very short C-C bond distances (approximately 1.26 Å) the propadienone structure has C_{2v} symmetry. As in the ketene case, we have chosen to follow the minimum-energy dissociation path by computing the CCSD/cc-pVDZ optimized structure at each value of the C-C distance leading to carbon monoxide and the lowest singlet state of vinylidene.

Figures 9, 10, and 11 plot the conventional and local MP2 and CCSD potential energy curves for breaking the central C-C bond of propadienone. In this case, the curve exhibits a total of ten discontinuities, including five near the

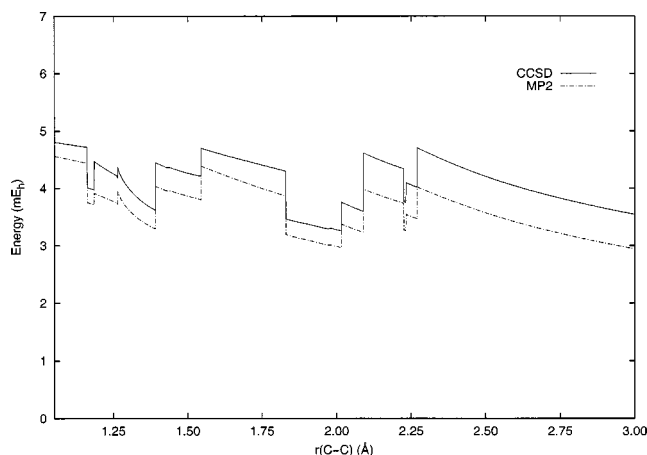


FIG. 12. LMP2 and LCCSD localization errors (in mE_h) for singlet propadienone dissociation, where the ten discontinuities discussed in the text are more clearly visible.

equilibrium geometry at 1.161, 1.185, 1.264, 1.390, and 1.544 Å, ranging in size from 0.1 to $0.8 mE_h$, and five in the bond breaking region at 1.829, 2.089, 2.225, 2.232, and 2.269 Å, ranging from 0.3 to $1.0 mE_h$, again on the same order as the localization error. As is evident from Fig. 12, which plots the localization error as a function of the central C-C distance, several of the discontinuities correspond to shifts back-and-forth in the orbital domain structures leading to a “jagged,” unphysical appearance to the PES.

VII. CONCLUSIONS

We have examined the occurrence of discontinuities in the potential energy surfaces given by the LMP2 and LCCSD local correlation methods based on the orbital domain approach of Pulay and Saebø. We find that for “pure” homolytic bond cleavage, as illustrated by breaking the C-F bond in fluoromethane, no such discontinuities appear due to the natural tendency of the Pipek–Mezey localized orbitals to remain delocalized between the separating fragments. On the other hand, for heterolytic bond cleavage and for shifts in the bond structure of conjugated systems, multiple discontinuities can occur, even in the vicinity of the equilibrium geometry, far from the bond-breaking regime. These discontinuities are usually small, but can often be of the same magnitude as the localization error (ca. $1 mE_h$), as illustrated above by singlet ketene and propadienone. The existence of such discontinuities prevents these types of local correlation models from adhering to the definition of a “theoretical model chemistry.”²⁸

ACKNOWLEDGMENTS

This work was supported by a National Science Foundation CAREER award (CHE-0133174), a Cottrell Scholar Award from the Research Corporation, a New Faculty Award from the Camille and Henry Dreyfus Foundation, the Jeffress

Memorial Trust, and a Lab-Directed Research and Development (LDRD) contract with the Department of Energy through Sandia National Laboratory (Livermore). The authors thank Professor Martin Head-Gordon (Berkeley) and Professor Marcel Nooijen (Waterloo) for helpful discussions.

- ¹ P. Pulay, *Chem. Phys. Lett.* **100**, 151 (1983).
- ² S. Saebø and P. Pulay, *Annu. Rev. Phys. Chem.* **44**, 213 (1993).
- ³ P. Pulay and S. Saebø, *Theor. Chim. Acta* **69**, 357 (1986).
- ⁴ S. Saebø and P. Pulay, *J. Chem. Phys.* **86**, 914 (1987).
- ⁵ M. Häser and J. Almlöf, *J. Chem. Phys.* **96**, 489 (1992).
- ⁶ P. E. Maslen and M. Head-Gordon, *Chem. Phys. Lett.* **283**, 102 (1998).
- ⁷ P. Y. Ayala and G. E. Scuseria, *J. Chem. Phys.* **110**, 3660 (1999).
- ⁸ M. Schütz, G. Hetzer, and H.-J. Werner, *J. Chem. Phys.* **111**, 5691 (1999).
- ⁹ C. Hampel and H.-J. Werner, *J. Chem. Phys.* **104**, 6286 (1996).
- ¹⁰ P. Maslen and M. Head-Gordon, *J. Chem. Phys.* **109**, 7093 (1998).
- ¹¹ M. Lee, P. Maslen, and M. Head-Gordon, *J. Chem. Phys.* **112**, 3592 (2000).
- ¹² P. E. Maslen, M. S. Lee, and M. Head-Gordon, *Chem. Phys. Lett.* **319**, 205 (2000).
- ¹³ G. E. Scuseria and P. Y. Ayala, *J. Chem. Phys.* **111**, 8330 (1999).
- ¹⁴ P. Constans, P. Ayala, and G. Scuseria, *J. Chem. Phys.* **113**, 10451 (2000).
- ¹⁵ G. Hetzer, M. Schütz, H. Stoll, and H.-J. Werner, *J. Chem. Phys.* **113**, 9443 (2000).
- ¹⁶ M. Schütz and H.-J. Werner, *J. Chem. Phys.* **114**, 661 (2001).
- ¹⁷ M. Schütz and H.-J. Werner, *Chem. Phys. Lett.* **318**, 370 (2000).
- ¹⁸ M. Schütz, *J. Chem. Phys.* **113**, 9986 (2000).
- ¹⁹ G. Rauhut and H.-J. Werner, *Phys. Chem. Chem. Phys.* **3**, 4853 (2001).
- ²⁰ M. Schütz, *J. Chem. Phys.* **116**, 8772 (2002).
- ²¹ M. Schütz, *Phys. Chem. Chem. Phys.* **4**, 3941 (2002).
- ²² M. Schütz and F. R. Manby, *Phys. Chem. Chem. Phys.* **5**, 3349 (2003).
- ²³ N. Flocke and R. J. Bartlett, *Chem. Phys. Lett.* **367**, 80 (2003).
- ²⁴ N. Flocke and R. J. Bartlett, *J. Chem. Phys.* **118**, 5326 (2003).
- ²⁵ S. Saebø and P. Pulay, *J. Chem. Phys.* **115**, 3975 (2001).
- ²⁶ J. Pipek and P. G. Mezey, *J. Chem. Phys.* **90**, 4916 (1989).
- ²⁷ J. W. Boughton and P. Pulay, *J. Comput. Chem.* **14**, 736 (1993).
- ²⁸ J. A. Pople, in *Energy, Structure, and Reactivity*, edited by D. W. Smith and W. B. McRae (Wiley, New York, 1973), pp. 51–61.
- ²⁹ N. R. Kestner, *J. Chem. Phys.* **48**, 252 (1968).
- ³⁰ J. H. van Lenthe, J. G. C. M. van Duijneveldt-van de Rijdt, and F. B. van Duijneveldt, *Adv. Chem. Phys.* **69**, 521 (1987).
- ³¹ S. F. Boys and F. Bernardi, *Mol. Phys.* **19**, 553 (1970).
- ³² S. Saebø, W. Tong, and P. Pulay, *J. Chem. Phys.* **98**, 2170 (1993).
- ³³ C. Möller and M. S. Plesset, *Phys. Rev.* **46**, 618 (1934).
- ³⁴ R. J. Bartlett, in *Modern Electronic Structure Theory*, Vol. 2 of *Advanced Series in Physical Chemistry*, edited by D. R. Yarkony (World Scientific, Singapore, 1995), Chap. 16, pp. 1047–1131.
- ³⁵ T. D. Crawford and H. F. Schaefer, in *Reviews in Computational Chemistry*, edited by K. B. Lipkowitz and D. B. Boyd (VCH Publishers, New York, 2000), Vol. 14, Chap. 2, pp. 33–136.
- ³⁶ T. D. Crawford, C. D. Sherrill, E. F. Valeev, J. T. Fermann, R. A. King, M. L. Leininger, S. T. Brown, C. L. Janssen, E. T. Seidl, J. P. Kenny, and W. D. Allen, *PSI 3.2*, 2003.
- ³⁷ T. D. Crawford and R. A. King, *Chem. Phys. Lett.* **366**, 611 (2002).
- ³⁸ T. H. Dunning, *J. Chem. Phys.* **90**, 1007 (1989).
- ³⁹ A. Dutta and C. D. Sherrill, *J. Chem. Phys.* **118**, 1610 (2003).
- ⁴⁰ W. D. Allen and H. F. Schaefer, *J. Chem. Phys.* **89**, 329 (1988).
- ⁴¹ S. K. Kim, Y. S. Choi, C. D. Pibel, Q.-K. Zheng, and C. B. Moore, *J. Chem. Phys.* **94**, 1954 (1991).
- ⁴² J. Yu and S. J. Klippenstein, *J. Phys. Chem.* **95**, 9882 (1991).
- ⁴³ W. H. Green, C. B. Moore, and W. F. Polik, *Annu. Rev. Phys. Chem.* **43**, 591 (1992).
- ⁴⁴ S. J. Klippenstein, A. L. L. East, and W. D. Allen, *J. Chem. Phys.* **101**, 9198 (1994).
- ⁴⁵ A. L. L. East, W. D. Allen, and S. J. Klippenstein, *J. Chem. Phys.* **102**, 8506 (1995).
- ⁴⁶ Q. Cui and K. Morokuma, *J. Chem. Phys.* **107**, 4951 (1997).
- ⁴⁷ A. L. L. East, *J. Chem. Phys.* **108**, 3574 (1998).